17 (2023) 100300

Contents lists available at ScienceDirect

International Journal of Thermofluids

journal homepage: www.elsevier.com/locate/ijtf

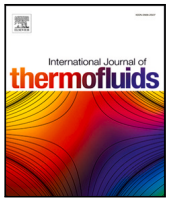

Two-step exothermic reaction–diffusion of hydromagnetic Prandtl–Eyring viscous heating fluid in a channel

Sulyman Olakunle Salawu

Department of Mathematics, Bowen University, Iwo, Nigeria

ARTICLE INFO

Keywords:
Prandtl–Eyring fluid
Two-step diffusion
Exothermic reaction
Viscous heating

ABSTRACT

The impact of toxic emission on the ecosystem and environmental degradation cannot be overstressed. This resulted from the rising incomplete hydrocarbon combustion of human activities. Thus, this study investigates temperature distribution of Prandtl–Eyring viscous heating fluid in a channel. A two-step exothermic reaction–diffusion of the viscoelastic fluid is assumed to enhance combustion process. Without reactant consumption, the fluid flow is pressure driven and influenced by an induced Lorentz force and pre-exponential factor. The model is governed by partial derivative equations subject to fixed walls and non-isothermal boundary conditions. A non-dimensional invariant model is obtained using dimensionless quantities, which is then solved by a semi-implicit difference method. The presented results in tables and graphs revealed that the second step exothermic reaction raised the heat distribution that assist in the complete combustion process. Also, the fluid viscosity is improved with rising material dilatant term. Hence, terms that induced heat generation should be guided to circumvent excessive heat that can lead to blowup.

1. Introduction

In recent decade, non-Newtonian fluids have been a major industrial working fluid due to their rheological properties and applications. These fluids are developed with different dynamical stress tensor, one of which is the Prandtl–Eyring fluid, Sreenivasulu [1]. The viscous fluid model is based on the topographical materialistic of strain rate hyperbolic function with slip stress linear relation [2–4]. It is used in PVC pipes, bulletproof jackets and in the production of polyvinyl chloride for the manufacturing of shoes, garments, hosepipe, insulator and many more, Qureshi [5]. Following Prandtl–Eyring fluid industrial usefulness in the presence of magnetic field, Munjam et al. [6] presented the flow of hydromagnetic Prandtl–Eyring radiative fluid along a stretchy convective heated plate. As mentioned, the viscous property of the magneto-fluid material is encouraged which leads to a damped velocity field. Salawu et al. [7] heat optimization of Prandtl–Eyring hybrid nanomaterial for nonlinear solar radiation absorber. It was reported that the solar heat distribution is increased with rising viscous material term. Hayat et al. [8] discussed the nanomaterial of Prandtl–Eyring melting thermal distribution and gyrotactic microorganism. The findings established that the temperature field intensified with an increased viscous dissipation and Prandtl terms. Rehman et al. [9] carried out transformation on heat and mass reaction–diffusion of Prandtl–Eyring liquid formulation using scaling group. The parametric sensitivity study shows that the diffusion–reaction of the chemical species is raised over the flow regime with rising material and viscous heating terms.

The species diffusion and heat transfer of non-Newtonian liquid material can be stimulated under exothermic generalized Arrhenius kinetics reaction. In industry and nature, large amount of heat is released from a system that undergoes exothermic reaction. In such a system, combustion process takes place [10–12]. The combustion process is essential in engineering and chemical sciences and useful in fire control and safety, pollution control, rocket propulsion, material processing and others, Ajadi [13]. An idealized one-step reaction–diffusion of exothermic has been investigated by many authors, among was Zhu et al. [14], in their study, an analytical analysis of premixed partial combustion for an effective radiative self-absorption. As revealed, heat radiation supports exothermic premixed reaction flame. Makinde [15] considered the thermal criticality of a thin film non-Newtonian third grade liquid flow driven by gravity along an adiabatic inclined channel. It was offered that the material term inspired internal combustion process of the fluid and excessive heat generation must be guided to mitigate system explosion. Salawu and Disu [16] studied a generalized Couette flow for one-step bifurcation and heat ignition of Oldroyd 6-constant liquid. The Frank-Kamenetskii and chemical initiation rate was reported to have greatly raised the temperature field. Hassan et al. [17] presented exothermic reaction of heat radiative and

E-mail address: issalawu.olakunle@bowen.edu.ng.

https://doi.org/10.1016/j.ijft.2023.100300
Received 7 October 2022; Received in revised form 15 January 2023; Accepted 1 February 2023
Available online 4 February 2023

generation of a hydromagnetic fluid flow in permeable channel media. An Arrhenius generalized kinetics was considered for the exothermic reaction and found that heat transfer is enhanced in the medium. More other useful findings and reports on one-step exothermic reaction can be found in [18–22]. Meanwhile, one-step diffusion–reaction assumptions is not sufficient to capture combustion reaction processes.

In a system where one-step exothermic reaction is not adequate, two-step exothermic reaction becomes the best option for the reaction combustion of materials, Salawu et al. [23]. For instance, automobile exhaust catalytic conversion in which complete hydrocarbon combustion is required, is a good platform for double exothermic reaction–diffusion, Szabo [24]. To reduce the toxic release of carbon II oxide that pollute and degrade environment, two-step exothermic reaction is encouraged to mitigate the ecosystem hazard, Makinde et al. [25]. A such, Kareem and Gbadeyan [26] presented heat ignition and entropy generation of two-step exothermic hydromagnetic combustion fluid flow in a generalized Couette channel. It was stated that the second step term raised temperature field to aid combustion reaction. Also, Salawu et al. [27] carried out theoretical analysis on the couple stress double exothermic diffusion–reaction and criticality in a channel in the presence of optical radiation and Reynolds viscosity. It was presented that the viscosity of lubricant material can be enhanced with rising non-Newtonian term and complete combustion is supported with rising second step term. Hence, the usefulness of two-step exothermic diffusion–reaction in thermal science and combustion technology cannot be overemphasized.

A two-step exothermic reaction–diffusion of non-Newtonian fluid has received little or no attention from the scientists, this has motivated the current research. Despite their essential and significant in improving lubricant oil, pollution control, jet and rocket propulsion and so on. Hence, the attention of this study has been focused on the two-step exothermic reaction–diffusion of hydromagnetic Prandtl–Eyring viscous heating fluid in a channel. The flow velocity and the temperature distribution of the double combustible fluid for various parameter sensitivities are carried out. The technological quantities, the skin friction and heat gradient are presented in table while the influence of entrenched terms are investigated graphically. A qualitative and quantitative solutions are done via semi-implicit finite difference for a comprehensive insight into the study.

2. Mathematical formulation

Consider a generalized Couette flow of hydromagnetic Prandtl–Eyring two-step exothermic combustion reactant. Without fluid reactant consumption, a viscoelastic Joule heating fluid is considered in a generalized chemical kinetic. The Prandtl–Eyring fluid undergoes double reaction–diffusion in a horizontal device. The fluid is pressure driven along a non-isothermal flow channel, and influenced by an electromagnetic induced force and pre-exponential factor n. Assuming z-axis direction is neglected, the flow material is in x-axis direction and y-axis considered perpendicular to it, as schematically demonstrated in Fig. 1.

The irreversible two-step exothermic combustion k-fluid for the species reactant oxidation is given as Williams [28]

$$C_2H_5OH + 2(94/25N_2 + O_2) \Longrightarrow 188/25N_2 + 2CO + 3H_2O$$

$$CO + 1/2(95/25N_2 + O_2) \Longrightarrow 47/25N_2 + CO_2$$

The compatible Prandtl–Eyring incompressible dynamical tensor stress is taken as [29,30]

$$\tau = \frac{\Lambda sin^{-1}\left\{\frac{1}{\alpha}\left[(\partial w_y)^2 + (\partial w_y)^2\right]^{1/2}\right\}}{\left[(\partial w_y)^2 + (\partial w_y)^2\right]}\partial w_y. \tag{1}$$

The mechanisms of the curving velocity is denoted as $\mathbf{W} = [\mathbf{w_1}(x, y, 0), \mathbf{w_2}(x, y, 0), 0]$, where Λ and α are the viscous fluid terms. The two-step temperature balance for combustible hydromagnetic exothermic reaction is taken as Salawu et al. [23,27]

$$\rho\partial T_t = -div\mathbf{q} + \Lambda(\nabla^2\mathbf{W})^2 + A_1H_1C_1 + A_2H_2C_2, \tag{2}$$

Here H_1 and H_2 represent the reaction heat, C_1 and C_2 denote species reactant, T is internal energy, $\mathbf{q}$ heat flux which from Fourier law takes the form $\mathbf{q} = -k\nabla T$ thermal conductivity, ρ is the density. According to [31,32], the reaction–diffusion temperature dependent rate A_1 and A_2 are given as,

$$A_1 = R_1\left(\frac{BT}{\upsilon\hbar}\right)^n e^{-E_1/RT}, \quad A_2 = R_2\left(\frac{BT}{\upsilon\hbar}\right)^n e^{-E_2/RT}, \tag{3}$$

where Planck's constant is $\hbar$, Boltzmann constant is B, R_1 and R_2 denote reaction order, E_1 and E_2 represent activation energy, vibration frequency is υ and n exponential factor i.e. $n \in \{-2, 0, 0.5\}$ for diverse kinetics. A Poiseuille flow boundary conditions are considered for the device configuration with isothermal thermal conditions. Assumed that the coefficient of reactant species consumption is small in the device, subject to the mentioned assumptions, the transient Powell-Eyring reactive flow rate and the temperature reaction balance according to [8,15,27] becomes:

$$\partial w_{\bar{t}} = -\partial\bar{p}_{\bar{x}} + \frac{\Lambda}{\rho\alpha}\partial^2 w_{\bar{y}\bar{y}} - \frac{\Lambda}{2\rho\alpha^3}\left(\partial w_{\bar{y}}\right)^2\partial^2 w_{\bar{y}\bar{y}} - \frac{\sigma B_0^2}{\rho}w, \tag{4}$$

$$\rho C_p\partial T_{\bar{t}} = k\partial^2 T_{\bar{y}\bar{y}} + \frac{\Lambda}{\alpha}\left(\partial w_{\bar{y}}\right)^2\left(1 - \frac{1}{6\alpha^2}(\partial w_{\bar{y}})^2\right) + \sigma B_0^2 w^2 + H_1C_1A_1 + H_2C_2A_2, \tag{5}$$

taking from [24,26], the applicable initial and boundary constraints are:

$$\begin{aligned} &w(\bar{y}, 0) = 0,\ T(\bar{y}, 0) = 0,\ w(0, \bar{t}) = 0,\ T(0, \bar{t}) = T_a,\ \partial w_{\bar{y}}(b, \bar{t}) = 0,\\ &T(b, \bar{t}) = T_0, \quad \text{for } \bar{t} > 0. \end{aligned} \tag{6}$$

The respective terms are velocity w, ambient temperature T_a, magnetic strength B_0, pressure p, initial temperature T_0, time $\bar{t}$, specific heat C_p, channel width b, electric conductivity σ and thermal conductivity k. With the subsequent suitable quantities, the dimensionless equations are obtained

$$\begin{aligned} &G = -\frac{\partial\bar{p}}{\partial\bar{x}}, t = \frac{\bar{t}\mu}{\rho b^2}, x = \frac{\bar{x}}{b}, u = \frac{w}{W_0}, \theta = \frac{E_1(T - T_0)}{T_0^2R},\\ &p = \frac{b\bar{p}}{W_0\mu}, y = \frac{\bar{y}}{b}, Br = \frac{E_1\mu W_0^2}{T_0^2Rk},\\ &a = \frac{E_2}{E_1}, \gamma = \frac{C_1H_1E_1R_1b^2}{kT_0^2R}\left(\frac{T_0B}{\hbar\upsilon}\right)^n e^{-\frac{1}{\lambda}}, \lambda = \frac{T_0R}{E_1},\\ &\beta = \frac{\Lambda}{\mu\alpha}, \delta = \frac{W_0}{2\alpha^2b^2}, \chi = \frac{C_2H_2R_2}{R_1C_1H_1},\\ &\theta_a = \frac{E_1(T_a - T_0)}{T_w^2R}, Pr = \frac{C_p\mu}{k}, H = \frac{\sigma B_0^2b^2}{\mu}. \end{aligned} \tag{7}$$

Applying the quantities of Eq. (7) on the dimensional partial derivative flow model and on the boundary conditions, the non-dimensional physical model is obtained as:

$$\partial u_t = G - \delta\beta\left(\partial u_y\right)^2\partial^2 u_{yy} + \beta\partial^2 u_{yy} - Hu, \tag{8}$$

$$Pr\partial\theta_t = \partial^2\theta_{yy} + \gamma\left\{(1 + \lambda\theta)^n\left(e^{\frac{\theta}{1+\lambda\theta}} + \chi e^{\frac{a\theta}{1+\lambda\theta}}\right)\right\} + Br\left[Hu^2 + \beta\left(\partial u_y\right)^2 - \frac{\delta\beta}{3}\left(\partial u_y\right)^4\right], \tag{9}$$

with the corresponding non-dimensional boundary constraints as

$$\begin{aligned} &u(0, t) = 0,\ u(y, 0) = 0,\ \theta(y, 0) = 0,\ \theta(0, t) = \theta_c,\\ &\partial u_y(1, t) = 0,\ \theta(1, t) = 0, \text{ for } t > 0. \end{aligned} \tag{10}$$

Table 1
Computed results for thermal criticality with different kinetics.

λ	χ	Br	Kinetics of $n = 0.5$		Kinetics of $n = 0$		Kinetics of $n = -2$	
			γ_{cr}	θ_{max}	γ_{cr}	θ_{max}	γ_{cr}	θ_{max}
0.1	0.0	0.0	3.307231	1.447599	3.823559	1.851517	7.644849	2.068259
0.1	0.0	0.2	3.210989	1.396427	3.666767	1.640554	9.063334	4.314019
0.2	0.7	0.5	1.786553	1.202721	2.009753	1.390478	3.868611	2.570552
0.2	0.5	0.0	2.204408	1.412590	2.548717	1.835072	5.077140	2.053736
0.3	0.5	0.2	2.140021	1.379997	2.444390	1.640554	6.042482	4.319192
0.3	1.0	0.5	1.443763	1.146831	1.607958	1.258885	2.809475	1.991306

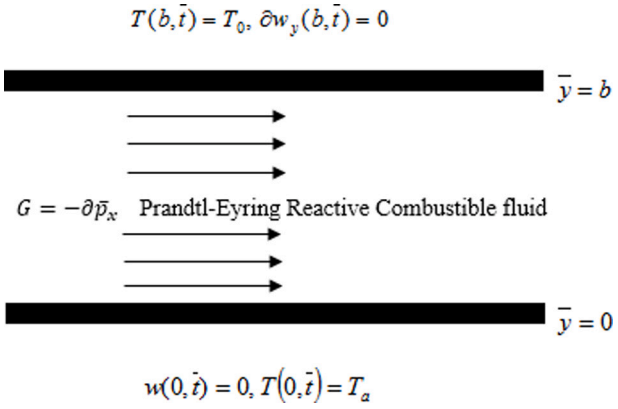

Fig. 1. Flow schematic configuration.

where the respective entrenched terms G, δ, β, H, Pr, γ, λ, χ, a and Br are pressure gradient, Prandtl–Eyring materials, magnetic term, Prandtl number, Frank-Kamenetskii, activation energy, reaction second step, activation energy ratio and Brinkman number. The dimensionless essential quantities of engineering consideration are the shear stress (Sr) and heat gradient (Hr) defined as:

$$Sr = \left(\beta \partial u_y - \frac{1}{3}\delta\beta[\partial u_y]^3\right)\Big|_{y=0}, \quad Hr = -\partial\theta_y\Big|_{y=0} \tag{11}$$

The comprehensive solutions of the transformed derivative models (8) to (11) are numerically computed to investigate the sensitivities of various emerging terms.

3. Numerical solution scheme

The numerical scheme is developed on a convergent and consistent semi-implicit finite difference method described in [33–35] for a non-isothermal viscoelastic fluid conditions. As [36,37] presented, the numerical algorithm is applied on reaction–diffusion of two-step non-Newtonian combustion reaction. An intermediate $(m + h)$ level of implicit time is adopted in the range $0 \le h \le 1$. In this study, $h = 1$ is considered to accommodate high computing time steps, which was used in Chinyoka [38]. An unvaried finite differences discretization in linear mesh and grid cartesian of the dimensionless partial derivatives model is done. An approximated spatial derivative is carried out by utilizing a second order central difference. As such, the integration of the resulting equations in grid point and the boundary constraints are executed. Thus, the momentum component in semi-implicit scheme is presented as

$$\frac{u^{(m+1)} - u^{(m)}}{\Delta t} = G - \delta\beta\partial u_y^{2(m)}\partial^2 u_{yy}^{(m+h)} + \beta\partial^2 u_{yy}^{(m+h)} - Hu^{(m+h)}, \tag{12}$$

here, $u^{(m+h)}$ in the equation is defined as

$$\begin{aligned} &-\xi_1 u_{j-1}^{(m+1)} + (2\xi_1 + 1)u_j^{(m+1)} - \xi_1 u_{j+1}^{(m+1)} = u^{(m)} + \Delta t(1-\xi)\beta u_{yy}^{(m)} \\ &- \Delta t\beta\delta(u_y)^{2(m)}u_{yy}^{(m)} + \\ &\Delta t G - \Delta t H u^{(m)}. \end{aligned} \tag{13}$$

where, $\xi_1 = \frac{\Delta t}{\Delta y^2}$. The solutions technique in $u^{(m+1)}$ transforms to an inverse tri-diagonal matrix, this gives a better result than a whole implicit scheme. Therefore, the heat propagation for the combustible fluid reaction in a semi-implicit scheme form follows after the velocity component. The partial second order derivative for the temperature module in semi-implicit form gives:

$$\begin{aligned} Pr\frac{\theta^{(m+1)} - \theta^{(m)}}{\Delta t} &= \theta_{yy}^{(m+h)} + \gamma(1+\lambda\theta)^n\left(e^{\frac{\theta}{1+\lambda\theta}} + \chi e^{\frac{a\theta}{1+\lambda\theta}}\right)^{(m)} \\ &+ Br\left(Hu^2 + \beta\left(\partial u_y\right)^2 - \frac{\delta\beta}{3}\left(\partial u_y\right)^4\right)^{(m)}, \end{aligned} \tag{14}$$

where $\theta^{(m+1)}$ is described as

$$\begin{aligned} &-\xi_2\theta_{j-1}^{(m+1)} + (2\xi_2 + Pr)\theta_j^{(m+1)} - \xi_2\theta_{j+1}^{(m+1)} \\ &= \Delta t Br\left(Hu^2 + \beta\left(\partial u_y\right)^2 - \frac{\delta\beta}{3}\left(\partial u_y\right)^4\right)^{(m)} + \\ &\Delta t\gamma(1+\lambda\theta)^n\left(e^{\frac{\theta}{1+\lambda\theta}} + \chi e^{\frac{a\theta}{1+\lambda\theta}}\right)^{(m)} + \theta^{(m)} + \Delta t\theta_{yy}^{(m)}, \end{aligned} \tag{15}$$

here, $\xi_2 = \frac{\Delta t}{\Delta y^2}$. The computational solution technique in $\theta^{(m+1)}$ gives an inverse tri-diagonal matrix. The numerical technique is confirmed for accuracy with $h = 1$ and established to be consistent in first and second order respectively in time and space. Therefore, the method of solution is presented for temporal and spatial convergence, it is proved to be independent of mesh and step sizes. The solution at $\Delta t = 1$ with 150 steps time are similar to that after 30 steps time at $\Delta t = 5$. Also, with $\Delta y = 0.02$ at $\Delta t = 0.05$ or $\Delta t = 0.025$ converges at the same outputs. The Maple code runs faster which enable steady state outputs at closed trivial computational times.

4. Results and discussion

The Prandtl–Eyring hydromagnetic two step combustion process has been analyzed using a semi-implicit finite difference technique. The method is adopted because of its stability, consistence, convergent and accuracy. Taking from the previous articles [5,12,13], the default term values are $G = 0.3$, $Br = 0.3$, $Pr = 3$, $\beta = 0.2$, $n = 0.5$, $\delta = 0.3$, $\chi = 0.5$, $a = 1$, $H = 0.7$, $\lambda = 0.3$, $\theta_c = 0$ and $\gamma = 0.1$ otherwise as shown in each plot. Table 1 displayed the thermal criticality computed results for different chemical kinetics, for which $n = 0.5$ depicts the Bimolecular kinetics, $n = 0$ denotes Arrhenius kinetics while $n = -2$ shows sensitized kinetics. The thermal combustion terms λ, χ and Br are investigated for the θ_{max} and γ_{cr}. As noticed, the sensitized kinetics produces higher values for the θ_{max} and γ_{cr}, follow by Arrhenius kinetics then by Bimolecular kinetics. The outcomes is been influenced by the fluid material and boundary layer conditions. Whereas, in Table 2, the wall friction and heat transfer gradient results are presented. As seen, some terms created an increasing effect while some reduced the wall effect. This could be traced to the strength of induced magnetic field, Ohmic heating and viscosity of the material. Table 3 depicts the comparison of the thermal criticality computed results with existing one. As seen, this established the authenticity and accuracy of the present results presented.

The response of the flow dimension field to an increase in the material non-Newtonian dilatant term (β) and magnetic term (H) are

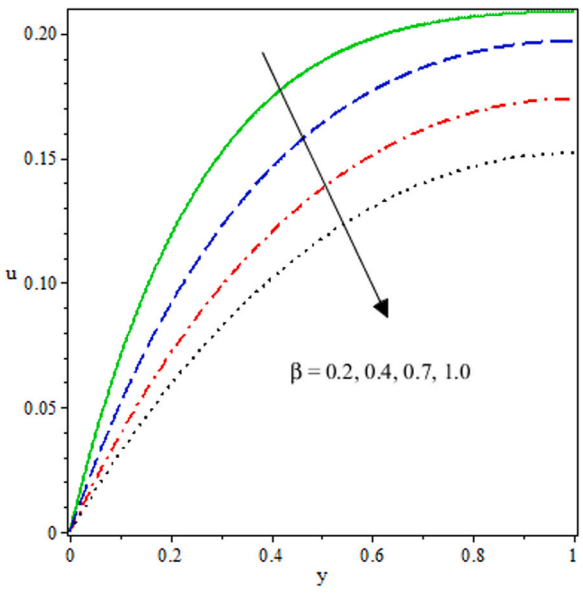

Fig. 2. Velocity distribution for various β.

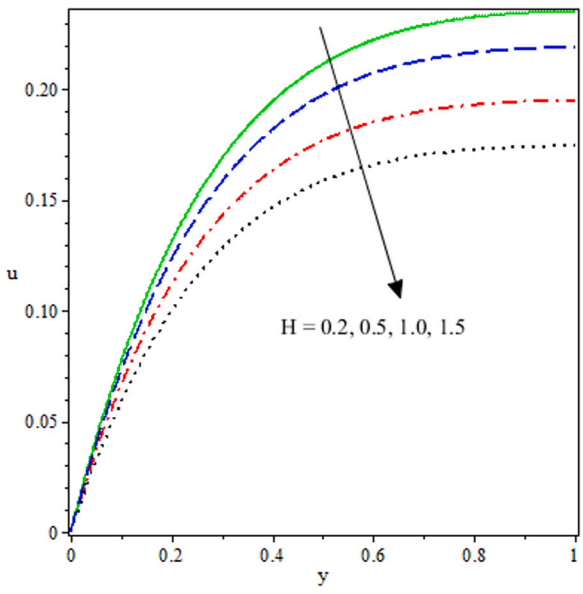

Fig. 3. Velocity field for different H.

Table 2
Computed outcomes for wall drag (Sr) and wall gradient (Hr).

H	λ	χ	γ	G	Sr	Hr
0.7	0.3	0.5	0.1	0.3	0.8064272086	0.0864398473
1.0					0.0680149172	0.0840103029
1.5					0.5563276261	0.0818279427
	0.1				0.0862222878	0.8064272086
	0.2				0.0863309014	–
		0.7			0.0968217967	–
		1.0			0.1124839370	–
			0.15		0.1256185998	–
			0.20		0.1654853598	–
				0.05	0.0765329919	0.1276016933
				0.20	0.0807744238	0.5208829695

respectively demonstrated in Figs. 2 and 3. As seen in Fig. 2, the Prandtl–Eyring term enhanced the combustible fluid viscosity, which resulted from the rising shear stain and shear thickness. This created the dispersion of a fluid particle in the suspended surface chemistry of the non-Newtonian material. As such, the fluid velocity is decreased progressively along the flow channel. Also, in Fig. 3, rising magnetic term values damped the fluid flow distribution in the isothermal bounded channel. The induced electromagnetic force stimulated by the magnetic field encouraged molecular bonding, this thereby dragged the velocity field as presented in the plot. This effect is significant in controlling free flow of the combustible fluid as the viscosity is raised to restrict fluid particles interaction. Hence, an induced Lorentz force opposes fluid velocity distribution. Fig. 4 denotes the impact of pressure gradient (G) on the velocity profile. As observed, the pressure is rapidly experienced at the upper part of the channel. The reaction–diffusion flow rate is raised gradually due to the stimulated Ohmic heating and internal heat generation that discouraged the fluid viscosity. This resulted in the overall rising in the free fluid particle propagation and in turn increase the flow velocity field. Moreover, the effect of pressure gradient (G) and magnetic term (H) are respectively offered in Figs. 5 and 6. The two parameters (G) and (H) propel heat source terms and exothermic reaction in the energy equation (9), which thereby damped the viscoplastic molecular bond. As such, the particle interaction is inspired to induce internal heating that leads to increasing temperature distribution in the system. In addition, the magnetic term induced Lorentz force that stimulates the Prandtl–Eyring viscoelastic property, this encouraged reaction–diffusion of the combustible fluid. Thus, the heat transfer rate is enhanced.

In Fig. 7, the influence of the second step term (χ) is demonstrated on the heat transfer profile. The temperature field is strongly increased with rising parameter numbers (χ). An increase in the temperature field is significant in enhancing complete combustion of hydrocarbon that can degrade the environment and ecosystem. As a result, double exothermic combustion of Prandtl–Eyring reactive fluid should be encouraged to reduce the release of carbon-monoxide to the surroundings. The reaction of heat distribution to a rising Brinkman number (Br) and Frank-Kamenetskii term (γ) are displayed in Figs. 8 and 9 respectively. Fig. 8 shows that the conducted heat from the flow medium wall to the viscous fluid increases along the channel. Hence, the molecular heat conduction from the viscous dissipation is enhanced to raise the temperature profile. Also, in Fig. 9, rising heat distribution is studied for the mixture of homogeneous reactants in a non-isothermal temperature. Thus, Frank-Kamenetskii term (γ) governed the ignition process of

Table 3
Comparison of thermal criticality computed outcomes with various kinetics.

λ	a	n	Makinde et al. [25]		Present results	
			θ_{max}	γ_c	θ_{max}	γ_c
0.1	0.1	0.5	1.42024388	0.93221607	1.42024400	0.93221675
0.1	0.1	0.0	1.58589905	0.95364522	1.58589889	0.95364492
0.1	0.1	−0.2	2.32077814	1.28209104	2.32077797	1.28209999
0.1	1.0	0.5	1.42024388	0.84746916	1.42024410	0.84746956
0.2	0.1	0.5	1.90527424	0.96808604	1.90527390	0.96808564
0.3	0.1	0.5	3.04684193	1.07442145	3.04684213	1.07442212

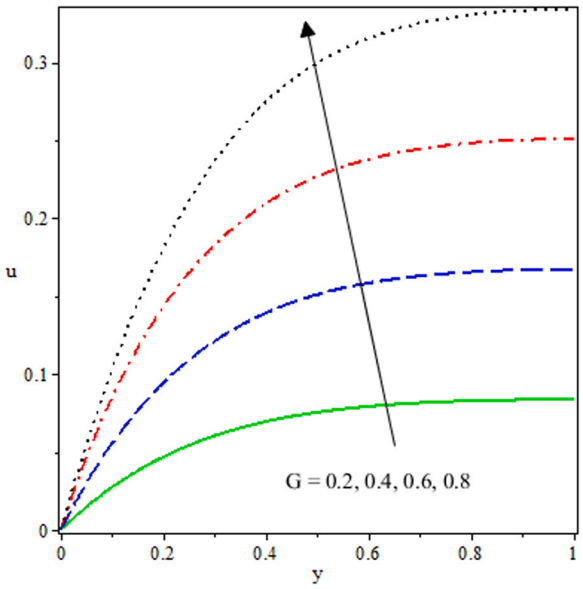

Fig. 4. Flow rate profile for increasing G.

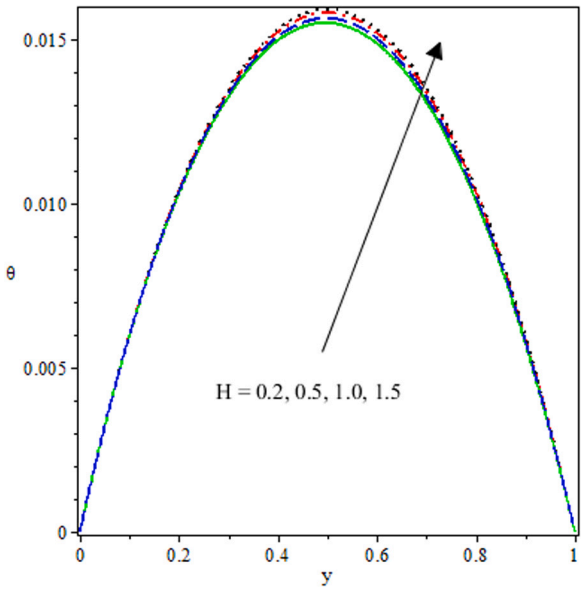

Fig. 6. Temperature field for rising H.

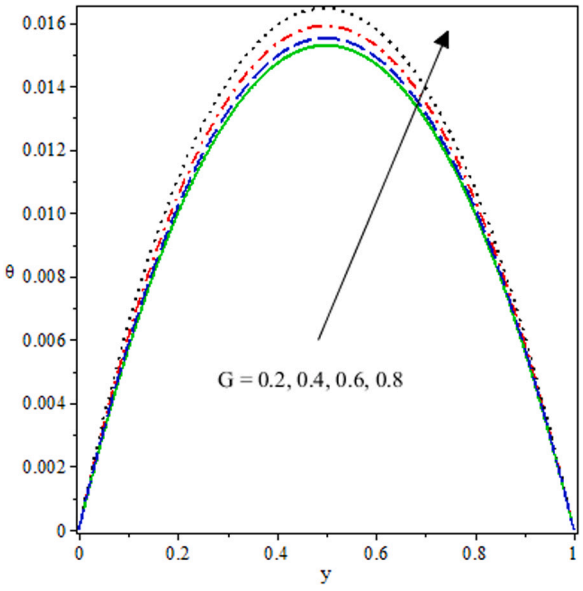

Fig. 5. Heat distribution for diverse G.

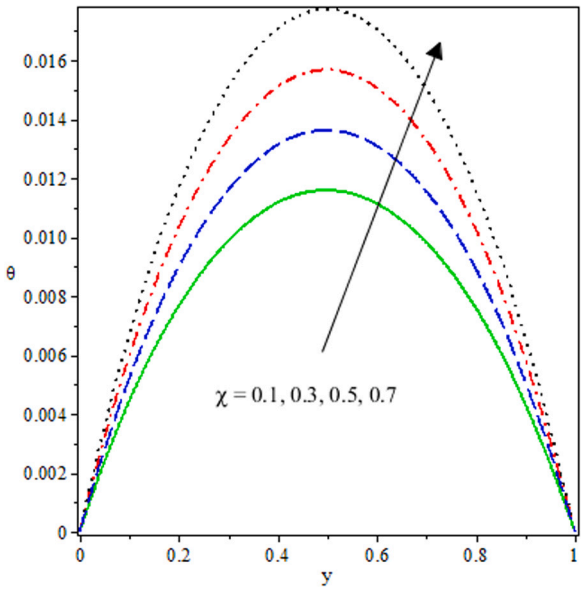

Fig. 7. Heat profile for increasing χ.

an exothermic chemical species, therefore reactant concentration consumption is assumed negligible for the considered bimolecular kinetics. Hence, in an exothermic two-step reaction–diffusion system, Frank-Kamenetskii term (γ) must be controlled to avoid thermal ignition. In Fig. 10, the effect of the activation energy ratio (a) on the exothermic heat propagation is demonstrated. The temperature profile increased with the rising ratio of the activation energy. Activation energy is the required energy to stimulate a reaction, thus the Prandtl–Eyring reactant molecules undergoes chemical transformation. The activation energy ratio induced heat energy, which inspired exothermic reaction temperature distribution along the flow channel. Increasing Prandtl number (Pr) is seen to have reduced temperature profile as presented in Fig. 11. The term (Pr) described the kinematic viscosity ratio to heat diffusion. As noticed, the momentum diffusivity dominates the two-step exothermic diffusion–reaction that leads to an enhanced kinematic viscosity. A such, heat generation is damped, thereby discourages temperature field as seen in the plot.

Conclusion

In the study, a two-step exothermic reaction–diffusion of hydromagnetic Prandtl–Eyring viscous heating fluid in a channel is examined. With appropriate transformation, the dimensionless model is obtained which represent the thermofluidic physical flow characteristics. The numerical solutions in graphs for the flow velocity and heat propagation are presented. Sensitivity of various embedded physical parameters is carried out. The summary of the findings are as follows:

- A monotonically rise in $u(y)$ along the flow stream y is damped with an increased dilatant material and magnetic terms.
- The flow rate and temperature field are raised to the peak along the middle of the channel for increasing pressure gradient.

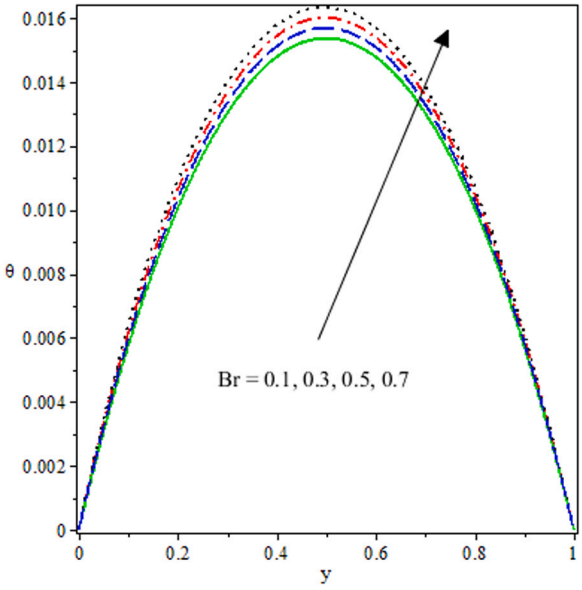

Fig. 8. Temperature profile for various *Br*.

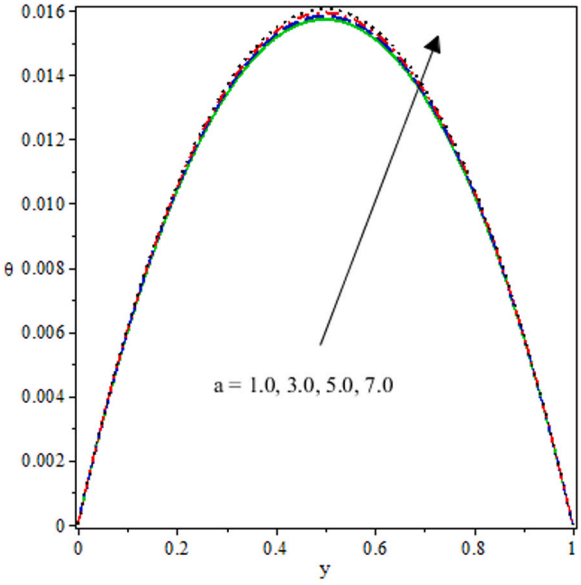

Fig. 10. Heat distribution for rising *a*.

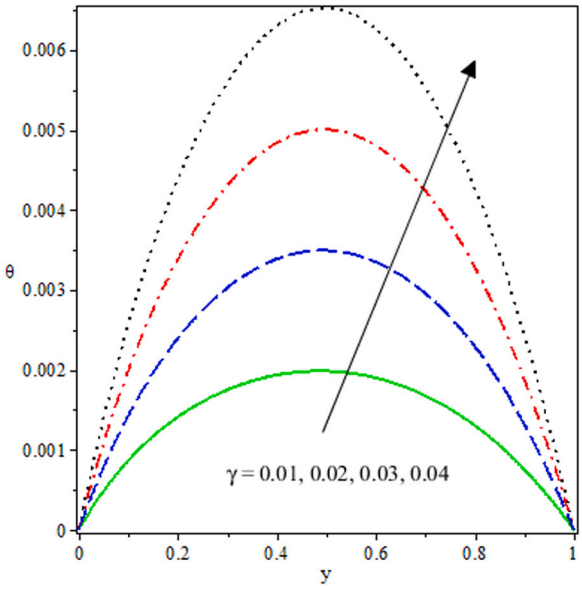

Fig. 9. Heat propagation for rising γ.

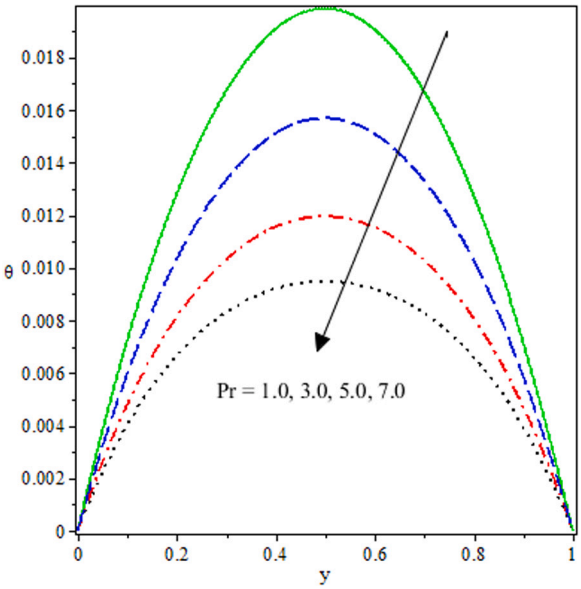

Fig. 11. Energy profile for increasing *Pr*.

- The Prandtl–Eyring combustion process is encouraged with rising Brinkman number, activation energy ratio and Frank Kamenetskii term.
- Second step term boosted the temperature distribution to support complete hydrocarbon combustion.

The study is useful in nature and industries that relies on the combustion process for their activities, such as power production, jet and rocket propulsion, fire prevention, pollution control, basic chemical reactive flow system and so on. Hence, extension to other non-Newtonian materials in annular cylinder is encouraged.

Declaration of competing interest

The authors declare that they have no known competing financial interests or personal relationships that could have appeared to influence the work reported in this paper.

Data availability

No data was used for the research described in the article.

References

[1] P. Sreenivasulu, T. Poornima, B. Malleswari, N.B. Reddy, B. Souayeh, Internal energy activation stimulus on magneto-bioconvective Powell-Eyring nanofluid containing gyrotactic microorganisms under active/passive nanoparticles flux, Phys. Scr. 96 (2021) 055221.

[2] R.M. Darji, M.G. Timol, Similarity solutions of leminar incompressible boundary layer equations of non-Newtonian viscoinelastic fluids, Int. J. Math. Ach. 2 (2011) 1395–1404.

[3] T. Hayat, S. Bibi, F. Alsaadi, M. Rafiq, Peristaltic transport of Prandtl-Eyring liquid in a convectively heated curved channel, PLoS One 11 (2016) e0156995.

[4] S.O. Salawu, A.M. Obalalu, M.D. Shamshuddin, Nonlinear solar thermal radiation efficiency and energy optimization for magnetizedhybrid Prandtl-Eyring nanoliquid in aircraft, Arab. J. Sci. Engin. 22 (2022) 070801.

[5] M.A. Qureshi, A case study of MHD driven Prandtl-Eyring hybrid nanofluid flow over a stretching sheet with thermal jump conditions, Case Stud. Therm. Engin. 28 (2021) 101581.
[6] S.R. Munjam, K. Gangadhar, R. Seshadri, M. Rajeswar, Novel technique MDDIM solutions of MHD flow and radiative Prandtl-Eyring fluid over a stretching sheet with convective heating, Int. J. Ambient Energy 17 (2021) 1–10.
[7] S.O. Salawu, A.M. Obalalu, E.O. Fatunmbi, R.A. Oderinu, Thermal Prandtl-Eyring hybridized MoS2-SiO2/C3H8O2 and SiO2-C3H8O2nanofluids for effective solar energy absorber and entropy optimization: A solar water pump implementation, J. Mol. Liquids 361 (2022) 119608.
[8] T. Hayat, I. Ullah, K. Muhammad, A. Alsaedi, Gyrotactic microorganism and bio-convection during flow of Prandtl-Eyring nanomaterial, Nonlinear Engin. 10 (2021) 201–212.
[9] K.U. Rehman, A.A. Malik, M.Y. Malik, M. Tahir, I. Zehra, On new scaling group of transformation for Prandtl-Eyring fluid model with both heat and mass transfer, Results Phys. 8 (2018) 552–568.
[10] P. Sreenivasulu, T. Poornima, B. Malleswari, N.B. Reddy, B. Souayeh, Viscous dissipation impact on electrical resistance heating distributed Carreau nanoliquid along stretching sheet with zero mass flux, Eur. Phys. J. Plus 135 (2020) 705.
[11] S.O. Salawu, S.S. Okoya, On criticality for a branched-chain thermal reactive-diffusion in a cylinder, Combust. Sci. Technol. 194 (9) (2022) 1815–1829.
[12] M.I. Afridi, A. Wakif, A.K. Alanazi, Z.M. Chen, M.U. Ashraf, M. Qasim, A comprehensive entropic scrutiny of dissipative flows over a thin needle featured by variable thermophysical properties, Waves Random Complex Media 17 (2022) 49922.
[13] S.O. Ajadi, Approximate analytic solution for critical parameters in thermal explosion problem, Appl. Math. Comput. 218 (2011) 2005–2010.
[14] X.L. Zhu, J.P. Gore, A.N. Karpetis, R.S. Barlow, The effects of self-absorption of radiation on an opposed flow partially premixed flame, Combust. Flame 129 (2002) 342–345.
[15] O.D. Makinde, Thermal criticality for a reactive gravity driven thin film flow of a third grade fluid with adiabatic free surface down an inclined plane, Appl. Math. Mech. 30 (3) (2009) 373–380.
[16] S.O. Salawu, A.B. Disu, Branch-chain criticality and thermal explosion of Oldroyd 6-constant fluid for a generalized Couette reactive flow, South Afr. J. Chem. Engin. 34 (2020) 90–96.
[17] A.R. Hassan, R. Maritz, J.A. Gbadeyan, A reactive hydromagnetic heat generating fluid flow with thermal radiation within porous channel with symmetrical convective cooling, Int. J. Therm. Sci. 122 (2017) 248–256.
[18] S.O. Adesanya, J.A. Falade, S. Jangili, O. Anwar Beg, Irreversibility analysis for reactive third-grade fluid flow andheat transfer with convective wall cooling, Alex. Eng. J. 56 (1) (2017) 153–160.
[19] J.H. Frank, R.S. Barlow, C. Lundquist, Radiation and nitric oxide formation in turbulent non-premixed jet flames, Proc. Combust. Inst. 28 (2000) 447–454.
[20] S.O. Salawu, A.B. Disu, M.S. Dada, On criticality for a generalized Couette flow of a branch-chain thermal reactive third-grade fluid with Reynolds's viscosity model, Sci. World J. 20 (2020) 10.
[21] W.L.b. Grosshandler, Radical: A narrow-band model for radiation calculations in a combustion environment, in: NIST Technical Note,Vol. 1402, 1993.
[22] S.S. Okoya, Computational study of thermal influence in axial annular flow of a reactive third grade fluid with nonlinear viscosity, Alex. Eng. J. 58 (1) (2019) 401.
[23] S.O. Salawu, A. Abolarinwa, O.J. Fenuga, Transient analysis of radiative hydromagnetic Poiseuille fluid flow of two-step exothermic chemical reaction through a porous channel with convective cooling, J. Comput. Appl. Res. Mech. Engin. 10 (1) (2020) 51–62.
[24] Z.G. Szabo, Advances in Kinetics of Homogeneous Gas Reactions, Methusen and Co Ltd, Great Britain, 1964.
[25] O.D. Makinde, P.O. Olanrewaju, E.O. Titiloye, A.W. Ogunsola, On thermal stability of a two-step exothermic chemical reaction in a slab, J. Math. Sci. 13 (2013) 1–15.
[26] R.A. Kareem, J.A. Gbadeyan, Entropy generation and thermal criticality of generalized couette hydromagnetic flow of two-step exothermic chemical reaction in a channel, Int. J. Thermofluids 5–6 (2020) 100037.
[27] S.O. Salawu, H.A. Ogunseye, M.D. Shamshuddin, A.B. Disu, Reaction–diffusion of double exothermic couple stress fluid and thermalcriticality with Reynolds viscosity and optical radiation, Chem. Phys. 561 (2022) 111601.
[28] F.A. Williams, Combustion Theory, second ed., Benjamin & Cuminy Publishing Inc.,Menlo Park, California, 1985.
[29] M.A. Qureshi, A case study of MHD driven Prandtl-Eyring hybrid nanofluid flow over a stretching sheet with thermal jump conditions, Case Stud. Therm. Eng. 28 (2021) 101581.
[30] K.S. Mekheimer, S.F. Ramadan, New insight into gyrotactic microorganisms for bio-thermal convection of Prandtl nanofluid over a stretching/shrinking permeable sheet, SN Appl. Sci. 2 (2020) 450.
[31] S.S. Okoya, Disappearance of criticality for reactive third-grade fluid with Reynolds's model viscosity in a flat channel, Int. J. Non-Linear Mech. 46 (2011) 1110–1115.
[32] S.O. Salawu, R.A. Kareem, R.A., M.D. Shamshuddin, S.U. Khan, Double exothermic reaction of viscous dissipative Oldroyd 8-constant fluid and thermal ignition in a channel, Chem. Phys. Lett. 760 (2020) 138011.
[33] O.D. Makinde, T. Chinyoka, Numerical investigation of transient heat transfer to hydromagnetic channel flow with radiative heat and convective cooling, Commun. Nonlinear Sci. Numer. Simul. 15 (2010) 3919–3930.
[34] O.D. Makinde, T. Chinyoka, Numerical study of unsteady hydromagnetic generalized Couette flow of a reactive third-grade fluid with asymmetric convective cooling, Comput. Math. Appl. 61 (2011) 1167–1179.
[35] M.S. Khan, M.A. Siddiqui, M.I. Afridi, Finite difference simulation of nonlinear convection in magnetohydrodynamic flow in the presence of viscous and Joule dissipation over an oscillating plate, Symmetry 14 (10) (2022) 1988.
[36] O.D. Makinde, Thermal stability of a reactive viscous flow through a porous-saturated channel with convective boundary conditions, Appl. Therm. Engng. 29 (2009) 1773–1777.
[37] M.I. Afridi, Z.M. Chen, M. Qasim, Numerical Chebyshev finite difference examination of Lorentz force effect on a dissipative flow with variable thermal conductivity and magnetic heating: Entropy generation minimization, ZAMM J. Math. Mech. 102 (12) (2022) e202200010.
[38] T. Chinyoka, Computational dynamics of a thermally decomposable viscoelastic lubricant under shear, J. Fluids Engin. 130 (12) (2008) 7.